Assessing The Accuracy Of Huygens Boxes For Flush Mounted Antenna Placement Applications From VHF Measurements

Zain Haider[1], Francesco Saccardi[2], FELLOW, AMTA and Lars J. Foged[2], FELLOW, AMTA
(1) MICROWAVE VISION GROUP, VILLEJUST, FRANCE
(2) MICROWAVE VISION GROUP, POMEZIA, ITALY

***Abstract*— This paper presents a study aimed at developing guidelines for generating accurate Huygens Boxes from low-frequency antenna measurements, particularly in the VHF/UHF range, for antenna placement analysis. In flush-mounted scenarios, it is standard practice to measure the source antenna on a finite ground plane and apply a pre-processing step, known as the Infinite Plane Boundary Condition (IPBC), to emulate the response over an infinite ground plane.**

For the first time, a simulation-based approach is used to quantify far-field reconstruction errors arising from three key limitations in applying IPBC at low frequencies, namely: the size of the Huygens Box, the dimensions of the ground plane, and the truncation of the scanning area. Among these, scanning area truncation is particularly critical, as IPBC requires radiation pattern data from both the upper and the lower hemispheres to effectively mitigate edge diffraction effects. While a ground plane of 5–7 wavelengths is typically recommended, such dimensions are often impractical at VHF due to physical constraints. This study investigates the impact of using a reduced ground plane down to one wavelength and less. Additionally, the influence of varying Huygens box sizes is examined to determine the necessary margin between the antenna and the box boundary.

The overall analysis is conducted using two RF sources: a single blade antenna and a 2-element blade antenna array. The accuracy of the IPBC method is evaluated in both free-space conditions and in a realistic aircraft model scenario.

***Index Terms*—antenna placement, equivalent currents, huygens box, low frequency, multiprobe system, VHF.**

I. INTRODUCTION

The Huygens box (HB) representation of measured antennas is an efficient and accurate way to perform antenna placement analysis in Computational Electromagnetic (CEM) solvers. This technique has been used successfully in antenna placement over electrically large and complex structures such as spacecrafts [1], satellites [2] and vehicles [3]. The measured Near Field (NF) or Far Field (FF) radiation pattern of the isolated antenna is used to compute Equivalent Currents (EQC) on a surface enclosing the antenna using inverse source method [4] implemented in the commercially available software INSIGHT developed by MVG [5]. The obtained equivalent current model of the antenna in the form of HB can be imported in a wide range of commercial CEM tools [6-11] to perform numerical simulations with the complex structures. This approach is very effective when the CAD model of the antenna is not provided by suppliers as it's protected by intellectual property. Another advantage of this approach is that it doesn't require large and costly measurement facilities as only the source antenna is measured without the complex structure.

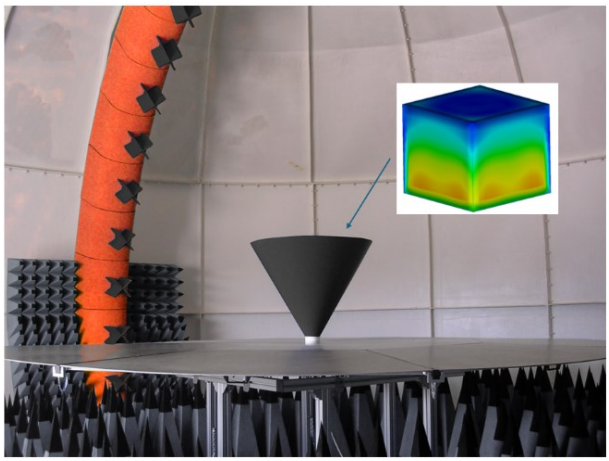

Figure 1: Example of a VHF/UHF multiprobe measurement system with 4m scanning radius and truncation of 20° below the horizon.

Flush mounted antennas scenarios pose additional challenges in the determination of the EQC model because the interaction with the metallic structure modifies the current distribution on the antenna itself. As a result, the standalone antenna cannot be considered during the measurements. Ideally, an infinite conductive Ground Plane (GP) should be considered at the bottom of the antenna which is to be placed on the final structure. However, this condition cannot be obtained in realistic measurement scenarios, but it can be approximated by performing antenna measurements on a finite GP [12-13]. Although, finite ground plane approximates correct local boundary condition, it also leads to diffraction from the edges of the finite ground plane. The diffractive contribution from the edges of the finite ground plane can be removed in a pre-processing step considering the so-called Infinite Plane Boundary Condition (IPBC) tool available in INSIGHT [12].

This paper reports on a study conducted to investigate the achievable accuracy for the generation of HB from low-frequency antenna measurements over finite ground planes. Implementing IPBC at low frequencies like VHF/UHF involves several challenges. First, using a finite ground plane that spans several wavelengths is physically impractical at VHF/UHF bands. Second, the standard λ/10 margin added to the HB often leads to a box size that is too large for practical antenna placement simulations. This margin is usually added to consider the uncertainty in the position of antenna during measurements. Third, spherical scan truncation, commonly occurring between 10° and 30° below the horizon in many low-frequency antenna measurement systems like the one shown in Figure 1 [14], further complicates the process. Therefore, the main objective of this study is to quantify the errors in far field reconstruction at low frequencies due to the size, shape of the ground plane, size of HB itself and the truncation of the scanning area.

This study employed a simulation-based approach to quantify the errors in far-field reconstruction arising from these limitations. The analysis is performed considering two types of source antennas, namely a blade antenna and a 2-element blade antenna array and an aircraft model intended to emulate a realistic antenna placement scenario.

The low-frequency spherical multiprobe system shown in Figure 1 represents a typical setup for VHF/UHF antenna measurements [14-15].These systems generally consist of two probe arrays covering the 70–400 MHz and 0.4–6 GHz frequency ranges, respectively. To keep the overall footprint compact and suitable for installation in relatively small and cost-effective anechoic chambers, such spherical NF systems typically feature a measurement radius between 4 and 6 m, with a truncated elevation scan ranging from the zenith down to 10°–30° below the horizon. The monocone antenna mounted on a circular ground plane, also depicted in Figure 1, illustrates a representative VHF measurement scenario using a limited-size ground plane (4m in diameter, or approx. 1.3 wavelengths at 100 MHz).

This paper is organized as follows. Section II presents the test cases along with the methodology adopted in this study. Section III shows the results and conclusions are drawn in section IV.

II. Simulation Workflow

In this section the adopted workflow used to perform the simulated analysis is described.

A. Source Antennas

The considered source antenna is the blade antenna (available in the open library of [8]) shown in Figure 2. The length and height of the antenna are approx. λ/6 and λ/5, respectively at operating frequency of 100 MHz. The antenna has been mounted over circular and square ground planes with a size ranging from λ/4 to 5λ. The antenna and ground plane has been modelled by perfect electric conductor (PEC) surface. The antenna has been fed by a discrete face port [6]. The blade antenna was selected based on its electrically small size. In addition, a two-element array of blade antennas has also been considered, where the distance between the center of two antennas was λ/2 as shown in Figure 2. Port 1 and port 2 of array were fed with an amplitude and phase of 1∠0° and 0.5∠30° respectively to obtain an asymmetric, and hence more challenging, antenna pattern.

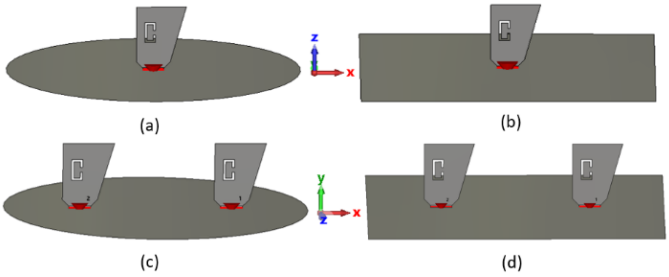

Figure 2: Test Cases (a) blade antenna over circular ground plane (b) blade antenna over square ground plane (c) blade antenna array over circular ground plane (d) blade antenna array over square ground plane

B. Infinite plane boundary condition

The IPBC emulates a radiation pattern over a virtual infinite ground plane from measurements (or simulations) performed on a finite ground plane. The diffractive contributions from the edges of the finite ground plane were removed by superposition of the far field pattern with its image. During the superposition, the diffraction from the edges cancels out as shown in Figure 3(a) and detailed in [11].

It is important to note that this process ideally requires the complete radiation pattern to be superimposed with its mirrored counterpart [16]. Incomplete or partial radiation patterns can lead to inaccuracies in diffraction cancellation. To assess the impact of such limitations, truncated datasets have been included in this study to quantify the effects of scan truncation.

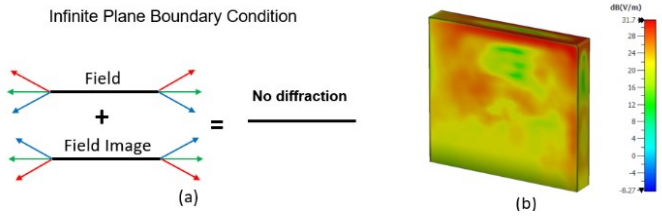

Figure 3: (a) Infinite plane boundary condition (b) Huygens box

C. Computation of Huygens box

After pre-processing to remove the edge diffraction, the far field patterns over virtual infinite ground planes have been used to compute HB enclosing the blade antenna and blade antenna array respectively.

The nominal dimension of the HB is 0.8m x 0.15m x 0.7m and 2.2m x 0.15m x 0.7m for antenna and array respectively. The HB for the blade antenna is shown in Figure 3(b).

D. Simulation of Complex Structure

The blade antenna and the blade antenna array have been placed over a CAD model of a generic aircraft and full-wave simulations have been performed as shown in Figure 4.

The length, width and height of the aircraft model were 71.7 m x 71.2 m x 21 m respectively. As can be seen, the antennas are positioned at the center of the fuselage. An integral equation solver [6] was used to perform numerical simulations with a mesh size of λ/10. These full-wave simulations have been performed to derive the reference radiation patterns for the analysis. In a second step, the HB of the two source antennas have been mounted in the same position of the antennas to perform the actual analysis.

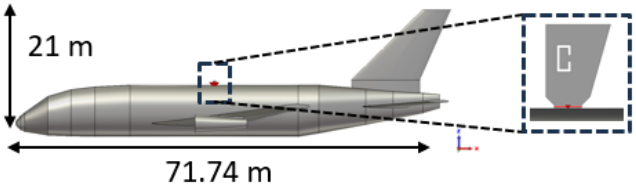

Figure 4: Antenna placement over CAD model of the aircraft.

E. Equivalent Noise Level

To quantify the accuracy of the far field patterns computed from the HB mounted on the aircraft, the Equivalent Noise Level (ENL) was computed:

$$ENL = 20log_{10}\left(RMS\left|\frac{E(\theta,\phi)-\tilde{E}(\theta,\phi)}{E(\theta,\phi)_{max}}\right|\right), \quad (1)$$

where $E(\theta,\phi)$ is the reference far field pattern and $\tilde{E}(\theta,\phi)$ is the far field pattern under analysis. The combinations reported in Table 1 have been considered to isolate the effect of each individual error contribution. In other words, the reference pattern and pattern under test differed only by one error term to isolate the errors.

Table 1. ENL combinations

ENL contribution	$E(\theta,\phi)$	$\tilde{E}(\theta,\phi)$
HB size	Full-wave simulation	HB from infinite GP + aircraft
GP size/shape	HB from infinite GP + aircraft	HB from finite GP + aircraft
Scan truncation	HB from 1λ GP + aircraft	HB from 1λ GP and scan truncation + aircraft

III. Results

The effect of each error term in the generation of HB and the subsequent simulation of the complex scenario is reported in this section.

A. Effect of Size of Huygens box

To quantify the effect of the size of the HB, the EQC reconstruction of the blade antenna at 100 MHz has been performed considering boxes of four different sizes. In this case the antenna has been simulated over an infinite conductive GP. The size of the HB has been increased in steps of 0.06λ. The directivity patterns computed from these HB mounted over the aircraft model are shown in Figure 5(a) for the cut plane ϕ=0° (i.e. the cut along the aircraft body). There is a good agreement of these directivity patterns with the directivity pattern computed from the full-wave simulation of the blade antenna over the aircraft model. Similar results were also obtained for the case of blade antenna array as shown in Figure 5(b). The visible pattern agreement was confirmed by evaluating ENL of directivity patterns with the reference directivity pattern from full wave simulation as shown in Figure 5(c). The ENL varied approx. between -49 dB to -45 dB by changing the HB margin from 0.02λ to 0.22λ. For the case of blade antenna array the ENL varied between approx. -42 dB to -39 dB as the HB margin varies from 0.01λ to 0.21λ.

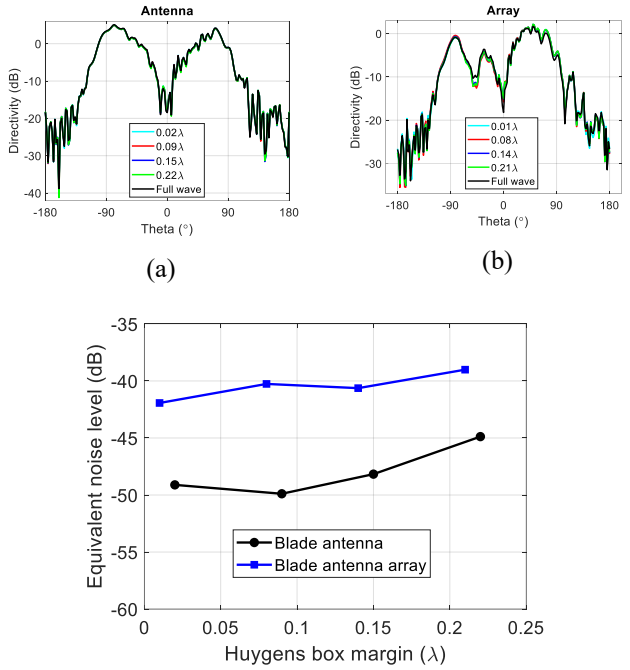

Figure 5: Far field pattern at 100 MHz (ϕ=0º) (a) blade antenna (b) blade antenna array (c) ENL

The increased complexity of the array antenna, compared to the standalone blade antenna, is likely the primary factor contributing to the higher observed ENL. For both source antennas, the ENL increased with the increase in the size of HB. This is likely due to the finite curvature of the fuselage, which creates a gap between the fuselage surface and the HB. The results showed that HB with margins less than λ/10 can be used at lower frequencies provided that the position of antenna is known with sufficient accuracy. Based on these results, we chose the HB with the smallest margin for both the blade antenna (0.02λ) and blade antenna array (0.01λ) for the rest of the analysis.

B. Effect of Size and Shape of Ground plane

1) IPBC results

To quantify the effect of size of the circular ground plane on application of IPBC, directivity patterns of the blade antenna and blade antenna array were obtained on ground planes of various

sizes (0.25λ - 5λ) as shown in Figure 6(a) and Figure 6(b) for cut plane ϕ=0°. After application of IPBC on these patterns, the resulting directivity patterns of blade antenna and blade antenna array over virtual infinite ground plane were obtained as shown in Figure 6(c) and Figure 6(d). The comparison of these directivity patterns with the reference directivity pattern obtained by full wave simulation of blade antenna and blade antenna array over infinite ground show a good agreement. For the blade antenna array over a 1λ ground plane, the higher deviation in the directivity pattern are due a the significant short distance from the antenna and the edge of the GP, being just λ/4; nonetheless, the overall agreement remains satisfactory, indicating the robustness of the approach. Similar results were also obtained for the case of square ground planes of various sizes (results not shown for brevity).

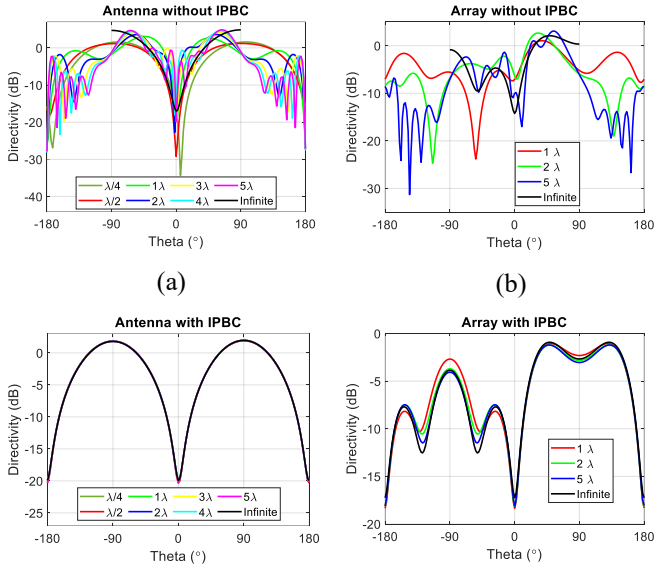

Figure 6: Far field pattern at ϕ=0º (a) blade antenna over circular ground plane without IPBC (b) blade antenna array over circular ground plane without IPBC (c) blade antenna over circular ground with IPBC (d) blade antenna array over circular ground

The ENL of the directivity patterns obtained from the IPBC applied to the simulation over the finite GPs against the simulation over the infinite GP are shown in Figure 7, for both source antennas, and both the circular and squared GPs. The results show that for both blade antenna and blade antenna array over circular ground planes, the ENL decreases with the increase in size of the ground plane after 1λ. In addition, there is a nonlinear trend of ENL when the size of the circular ground plane is less than 1λ. Although, the ENL of square GP was less regular than that of the circular ground plane, shape of the ground plane didn't show a significant effect on ENL, suggesting that both ground plane shapes could be used.

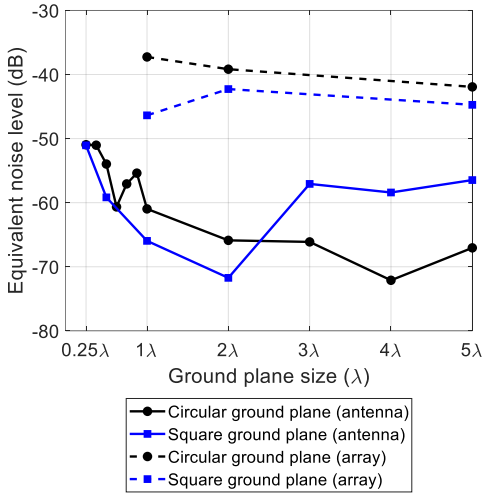

Figure 7: ENL in free-space. Simulated infinite GP vs. finite GP processed with the IPBC tool.

2) HB installed on the aircraft

The HB generated from aforementioned radiation patterns over virtual infinite GPs have been mounted over the fuselage of CAD model of the aircraft to test their accuracy in a realistic and complex scenario.

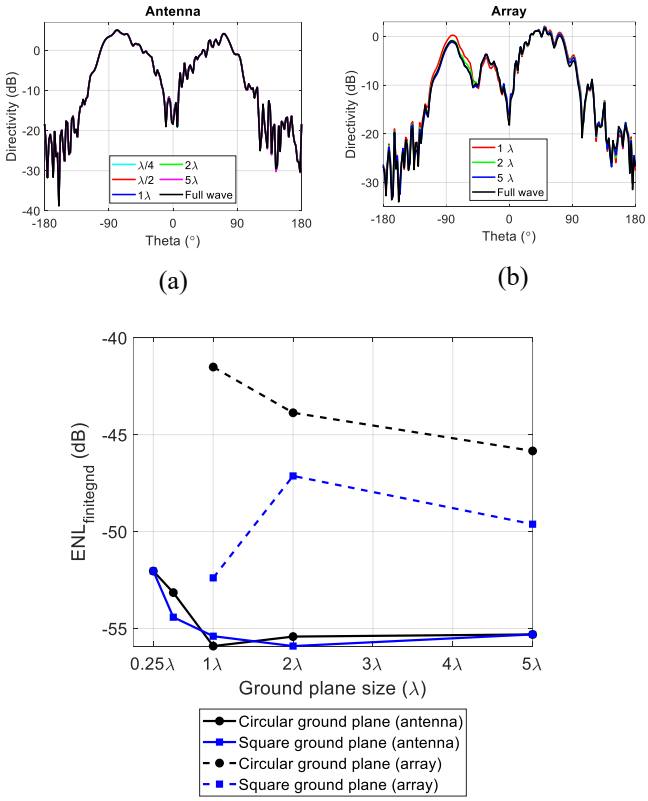

Figure 8: Far field pattern at 100 MHz (ϕ=0º) (a) blade antenna over circular ground plane (b) blade antenna array over circular ground plane (c) ENL

The directivity patterns computed from these HB for the case of blade antenna and blade antenna array are shown in Figure 8(a) and Figure 8(b) for cut plane ϕ=0°. The agreement of these directivity patterns with the reference pattern from full wave simulations is very good. Results for square ground planes are similar but are not shown for the sake of brevity. The ENL of these directivity patterns has been computed with the reference pattern obtained from HB over aircraft model generated from blade antenna over infinite ground plane. This is done to isolate the effect of the finite ground plane. As expected, Figure 8 (c) shows that the ENL decreases with the increase in size of the circular ground plane. Such obtained results suggest that 1λ GP is sufficient for accurate analysis in case of electrically small antennas (e.g. the blade antenna). On the other hand, the 1λ GP considered with the electrically larger antenna (the blade array antenna) gave rise to some higher errors. This suggests that the size of the GP should be at least 1λ larger than the size of the antenna (1.5-2λ in total in this case).

C. *Effect of Truncation*

1) IPBC results

To investigate the effect of the truncation of the scanning range, Spherical NF (SNF) measurements of a typical automotive measurement facility, like the one shown in Figure **1**, has been emulated considering a measurement radius of 4 m and the blade antenna over 1λ ground plane. Although the typical truncations of such systems range from 10° to 30° below the horizon (i.e. from θ=0° to θ=100°/120°), truncations from the horizon itself (i.e. θ=90°) to 70° below it (i.e. θ=160°) have been considered.

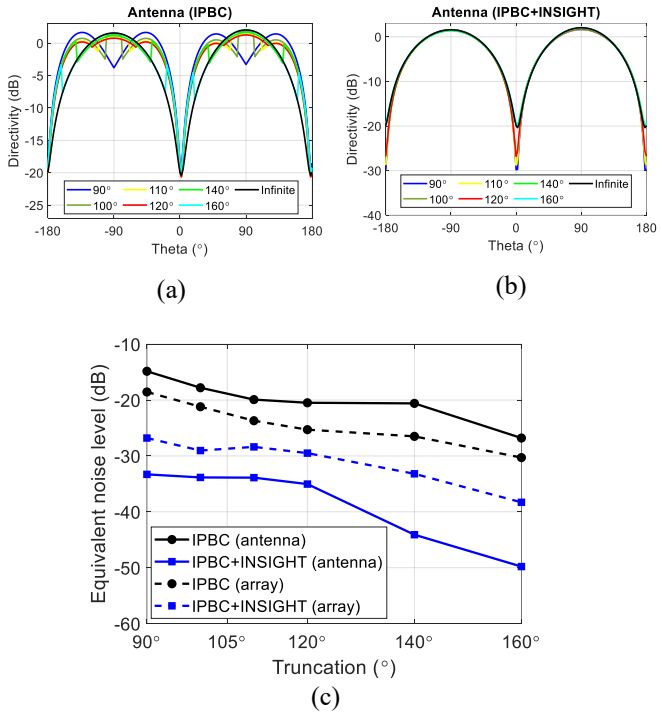

Figure 9: (a) IPBC (ϕ=0º) (b) IPBC + INSIGHT (ϕ=0º) (c) ENL

Figure 9(a) shows the directivity patterns after application of IPBC on the SNF data, while Figure 9(b) shows directivity patterns after application of IPBC and processing with the EQC technique. Similar results were obtained for the case of blade antenna array over 1λ ground plane (results not shown for brevity). The ENL of these patterns was computed with the reference directivity pattern obtained from full wave simulation of blade antenna and blade antenna array over an infinite ground plane. Figure 9(c) shows that ENL decreases with decrease in truncation and significantly it improves after field reconstruction with the EQC technique (blue traces).

1) HB installed on the aircraft

The directivity patterns obtained from the HB computed considering the different scan truncations, and then mounted on the aircraft model are shown in Figure 10(a) and Figure 10(b) for the two source antennas for cut plane ϕ=0°.

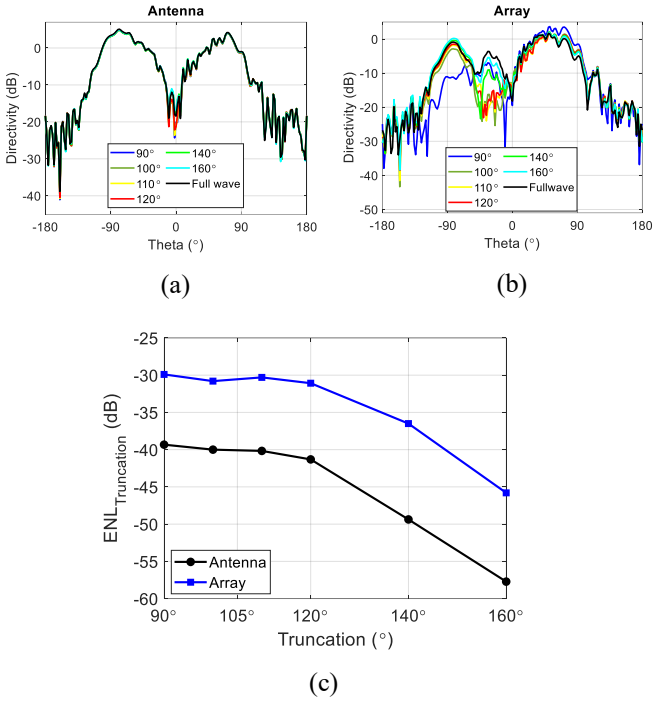

Figure 10: Far field pattern at ϕ=0º with truncation effect: (a) blade antenna over 1λ ground plane; (b) blade antenna array over 1λ ground plane (c) ENL.

The directivity patterns for the case of blade antenna show good agreement with the reference pattern from full wave simulations. For the blade antenna array, truncations with θmax<140° exhibit noticeable deviations from the reference pattern within a limited angular sector between –45° and 0°; nevertheless, an overall good reconstruction of the radiation pattern is achieved despite the significant scan truncation and size of the GP. The further degraded performance obtained with the hemispherical truncation (θ_{max}<90°, blue trace) are expected, as the IPBC method relies on superimposing image pattern to the original pattern to cancel edge diffraction. Due to the limited common area between the two patterns, the edge diffraction cannot be effectively canceled during the superposition process.

The ENL of these directivity patterns was computed with reference pattern obtained from HB over aircraft model generated from blade antenna over 1λ ground plane without truncation. This is to isolate the effect of the truncation. Figure 10(c) shows that the ENL decreases with decreasing truncation angle. Despite the lack of significant information in the lower hemisphere, it can be seen that typical scan truncations at θ=110° can give rise to relatively low ENL (-40dB and -30dB respectively for the blade antenna and the array). It is pointed out that the performance can be further improved by moving the antenna up during measurements to reduce the portion of the radiated power falling in the truncated region.

D. Summary

Table 2 reports the ENL due the various error sources. The results show that scan truncation error is dominant error followed by the error due to the size of the HB and the lowest error is due to the size of the ground plane.

For the case of blade antenna, the Root Square Summation (RSS) of the errors due to size of the HB (-49.1 dB), finite size (1λ) of the circular ground plane (-55.9 dB) and scan (110°) truncation (-40.2 dB) gives a combined error of approx. -39.5 dB. Similarly, the RSS combined error for the array antenna is approx. -29.5dB.

Table 2. Summary

Error Sources	Blade antenna ENL	Blade antenna array ENL
Huygens box size	-49.1 dB (0.8 x 0.15 x 0.7 m)	-41.9 dB (2.2 x 0.15 x 0.7 m)
Finite ground plane (1λ) Circular ground plane	-55.9 dB	-41.5 dB
Finite ground plane (1λ) Square ground plane	-55.4 dB	-52.4 dB
Scan truncation (100º) Circular ground plane	-40 dB (1λ GP)	-30.8 dB (1λ GP)
Scan truncation (110º) Circular ground plane	-40.2 dB (1λ GP)	-30.3 dB (1λ GP)

IV. CONCLUSIONS

This study established practical guidelines for generating accurate Huygens box from low-frequency (VHF/UHF) antenna measurements using a simulation-based approach. We quantified reconstruction errors due to three key IPBC limitations: HB size, ground plane size, and scanning area truncation. The analysis, performed using single and dual-element blade antennas, was validated in both free-space and realistic aircraft scenarios, providing a foundation for practical low-frequency antenna placement analysis.

Although scan truncation emerged as the dominant source of error, the EQC processing technique proved effective in mitigating its impact. Notably, even substantial truncations, such as those extending to 20° below the horizon, resulted in relatively low residual errors, often reaching –30 dB or lower depending on the antenna type. Furthermore, this performance can potentially be enhanced by introducing a vertical offset during measurements, thereby maximizing the captured radiated power.

The study also demonstrates that Huygens Boxes with margins smaller than λ/10 can be effectively used at lower frequencies, provided the antenna position is known with sufficient accuracy. Specifically, margins of 0.02λ and 0.01λ for the blade antenna and the blade antenna array resulted in ENL values of –49 dB and –42 dB, respectively. The benefit of using smaller margins is particularly noteworthy, as it offers greater flexibility in antenna placement simulations.

Finally, the study demonstrates that a ground plane of at least one wavelength larger than the antenna should be selected to achieve accurate reconstructions. At VHF, this corresponds to approximately 3–4m, which remains feasible within typical low-frequency antenna measurement setups [14-15].

These encouraging results confirm the effectiveness of the HB technique based on the IPBC for flush-mounted antennas, even at low frequencies. While the application of the HB approach at VHF presents additional challenges, we have provided practical guidelines to enhance accuracy and to quantify the expected errors. As a next step, the focus will shift to evaluating the field at a closer distance instead of the far field radiation pattern and generalizing the methodology by considering alternative antenna positions within the aircraft and/or different complex structures.

REFERENCES

[1] L. J. Foged and al., “Feasibility and Accuracy of Antenna Placement Analysis based on Measured Sources and Commercial Numerical Tools ”, Antenna Testand Measurement Society conference, 2015.

[2] M. Saporetti L. Scialacqua F. Saccardi L.J. Foged, J. Zackrisson, “Improved Measured Source Antenna Representation in Satellite Antenna Placement Analysis with Numerical Simulation ”, 2018 IEEE International Symposium on Antennas and Propagation, Boston, Massachusetts, USA - 8–13 July 2018.

[3] P. W. Futter, L. Scialacqua, L. J. Foged, J. Soler, “Automotive Antenna Placement and EMC Analysis Combining Measurement with Simulation ”, 2017 Asia-Pacific International Electromagnetic Compatibility (APEMC) Symposium in Seoul, Korea, June 20–23, 2017.

[4] L. Araque Quijano, G. Vecchi, " Improved accuracy source reconstruction on arbitrary 3-D surfaces. Antennas and Wireless Propagation Letters, IEEE, 8 : 1046–1049, 2009.

[5] INSIGHT software : https://www.mvg-world.com/en/products/antenna-measurement/software/insight

[6] https://www.3ds.com/products/simulia/cst-studio-suite (accessed July 2025)

[7] https://www.ansys.com/products/electronics/ansys-hfss (accessed July 2025)

[8] https://altairengineering.fr/feko/ (accessed July 2025)

[9] https://www.idscorporation.com/pf/space-electromagnetic-solutions/ (accessed July 2025)

[10] https://www.ansys.com/products/electronics (accessed July 2025)

[11] https://wipl-d.com/ (accessed July 2025)

[12] L. J. Foged, F. Mioc, B. Bencivenga, M. Sabbadini, E. Di Giampaolo, “Infinite ground plane antenna characterization from limited groundplane measurements ”, Antennas and Propagation Society International Symposium APSURSI, 17-July 11 2010.

[13] Chi-Chi Chen et al. “In Situ Response of Complex Antennas on Complex Platforms” AMTA 2024, Cincinnati, OH, US

[14] https://www.mvg-world.com/en/products/antenna-measurement/multi-probe-systems/sg-3000

[15] F. Saccardi, A. Giacomini, N. Gross, T. Blin, P.O. Iversen, L. J. Foged, “VHF/UHF Antenna Measurements Based on Multi Probe Array Technology” EuCAP 2024, Glasgow, Scotland.

[16] F. Saccardi, F. Mioc, A. Giacomini, L. J. Foged, "Estimation of the Realistic Ground Effect in Free-Space Automotive Measurements", AMTA 2018, 4-9 November, Williamsburg, Williamsburg, VA, USA